

Reduction of Systematic Uncertainty in DFT Redox Potentials of Transition-Metal Complexes

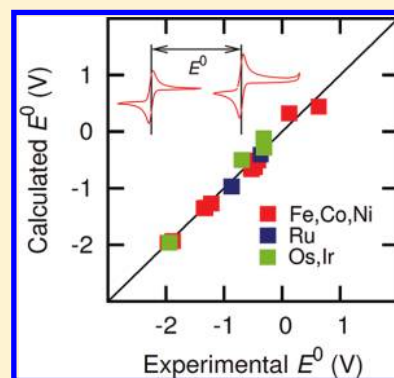
Steven J. Konezny,^{*,†} Mark D. Doherty,[‡] Oana R. Luca,[†] Robert H. Crabtree,[†] Grigorii L. Soloveichik,[‡] and Victor S. Batista^{*,†}

[†]Department of Chemistry, Yale University, P.O. Box 208107, New Haven, Connecticut 06520-8107, United States

[‡]General Electric Global Research, One Research Circle, Niskayuna, New York 12309, United States

S Supporting Information

ABSTRACT: Reliable calculations of redox potentials could provide valuable insight into catalytic mechanisms of electrochemically active transition-metal complexes as well as guidelines for the design of new electrocatalysts. However, the correlation between theoretical and experimental data is often uncertain, since redox properties depend strongly on experimental conditions of electrochemical measurements, including the nature of the solvent, electrolyte, and working electrode. Here, we show that the use of internal references allows for quantitative theoretical predictions of redox potentials with standard deviations σ comparable to typical experimental errors of cyclic voltammetry measurements. Agreement for first-, second-, and third-row transition-metal complexes is demonstrated even at a rather modest level of density functional theory ($\sigma = 64$ mV for the UB3LYP/6-311G* level). This is shown for a series of benchmark redox couples, including $[\text{MCp}_2]^{0/+}$ (Cp = η^5 -cyclopentadienyl), $[\text{MCp}^*_2]^{0/+}$ (Cp* = η^5 -1,2,3,4,5-pentamethylcyclopentadienyl), $[\text{M}(\text{bpy})_3]^{2+/3+}$ (bpy = 2,2'-bipyridine), and $[\text{Ir}(\text{acac})_3]^{0/+}$ (acac = acetylacetonate), with M = Fe, Co, Ni, Ru, Os, or Ir in various nonaqueous solvents [acetonitrile (MeCN), dimethyl sulfoxide (DMSO), and dichloromethane (DCM)].



1. INTRODUCTION

Accurate predictions of the electrochemical properties of transition metal complexes could provide valuable insight into catalytic mechanisms of electrocatalysts in a wide range of practical applications, including renewable energy technologies. Standard methods for computations of redox potentials are commonly applied in electrochemical studies,^{1–16} although methodologies that could account for systematic uncertainties of experimental or computational origin have yet to be established. This paper explores a practical, yet rigorous, approach that allows for quantitative predictions of redox potentials of transition metal complexes. The method reduces systematic errors that result from the theoretical approach (i.e., the choice of DFT functional, basis set, and solvation model) as well as the electrochemical measurement conditions, including the nature of the solvent, electrolyte, and working electrode. Therefore, this method should be particularly useful for reliable correlations between experimental and theoretical data.

Earlier reports typically documented deviations between experimental and theoretical values of redox potentials in the 150–540 mV range for most of the available methodologies.^{1–9} While these deviations continue to stimulate the development of more sophisticated DFT functionals, basis sets, and solvation models, we note that deviations in the documented experimental data can often be a major factor in accounting for discrepancies of comparable magnitude. This is largely due to the fact that redox properties are typically quite sensitive to the particular choice of solvent, electrode, or electrolyte conditions.

Therefore, identifying and reducing these sources of error is critical in establishing the capabilities and limitations of existing methods as well as for the design of new computational approaches. This paper explores a systematic methodology to remove uncertainties that are commonly included in comparisons between experimental and theoretical redox potentials, typically reported relative to external reference couples, or reference electrodes. We study benchmark redox couples, including complexes that span three transition metal rows in various nonaqueous solvents. It is shown that the use of appropriate references, measured under the same conditions and calculated by using compatible computational frameworks, allows for quantitative correlations between experimental and theoretical data. Such an approach leads to DFT redox potentials with standard deviations σ comparable to the experimental errors of cyclic voltammetry measurements, even at a rather modest level of theory (e.g., $\sigma = 64$ mV for the UB3LYP/6-311G* level).

This manuscript is organized as follows. In section 2, we discuss the origins of systematic error in comparisons of experimental and theoretical redox potentials. This discussion is followed by an outline of experimental and theoretical methods in sections 3 and 4. In section 5, benchmark results for various levels of theory are presented and discussed (section 5.1),

Received: January 15, 2012

Revised: February 18, 2012

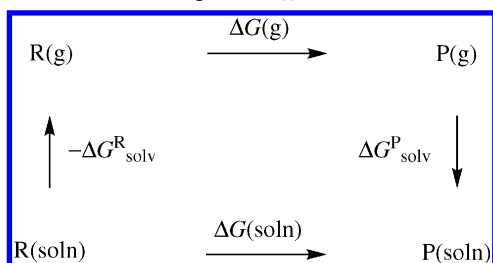
Published: February 21, 2012

followed by discussions on the choice of a reference redox system (section 5.2), the effects of solvent polarity and supporting electrolyte (section 5.3), and the chosen benchmark systems (section 5.4). A summary of conclusions is provided in section 6.

2. EXPERIMENTAL AND COMPUTATIONAL REDOX POTENTIALS

The absolute potential of a redox couple is typically computed from the Gibbs free energy change $\Delta G(\text{soln})$, associated with the reduction of R to form P in solution (see Scheme 1), as follows:

Scheme 1. Thermodynamic Cycle Used for the Calculation of Changes in Free Energy in Solution $\Delta G(\text{soln})$ from States R to P Based on Gas-Phase Minimum-Energy Geometries and Solvation Free Energies ΔG_{solv}



$$E_{\text{calc}}^{\text{abs}} = -\frac{\Delta G(\text{soln})}{nF} \quad (1)$$

where F is the Faraday constant, n is the number of moles of electrons involved in the redox reaction, and $\Delta G(\text{soln}) = \Delta G(\text{g}) + \Delta G_{\text{solv}}^{\text{P}} - \Delta G_{\text{solv}}^{\text{R}}$. For comparison with electrochemistry measurements, the resulting values are usually reported relative to a reference electrode (RE), such as the standard hydrogen electrode (SHE) or the saturated calomel electrode (SCE):

$$E_{\text{calc}}^0(\text{V vs RE}) = E_{\text{calc}}^{\text{abs}}(\text{V}) - E_{\text{calc,RE}}^{\text{abs}}(\text{V}) \quad (2)$$

Experimental redox potentials are typically reported with respect to a reference redox couple (RC), such as ferrocene/ferrocenium ($[\text{FeCp}_2]^{0/+}$):

$$E_{\text{exp}}^0(\text{V vs RC}) = E_{\text{exp}}^0(\text{V vs RE}) - E_{\text{exp,RC}}^0(\text{V vs RE}) \quad (3)$$

Therefore, comparisons between calculated $E_{\text{calc}}^0(\text{V vs RE})$ and experimental $E_{\text{exp}}^0(\text{V vs RE})$ values rely upon accurate potentials of reference electrodes $E_{\text{exp,RE}}^{\text{abs}}(\text{V})$ and reference redox couples $E_{\text{exp,RC}}^0(\text{V vs RE})$. However, the experimental values of typical reference electrodes (e.g., $E_{\text{exp,SHE}}^{\text{abs}}$ or $E_{\text{exp,SCE}}^{\text{abs}}$) vary by hundreds of millivolts from solvent to solvent, or from experiment to experiment with the same solvent but different electrolytes (Table 1). Furthermore, the configuration of the SCE typically generates a liquid junction potential that may or may not be reproducible in a given experiment. In general, nonaqueous reference electrodes based on the same solvent are prone to issues of reproducibility, which are often a result of electrode surface chemistry.²¹ In addition, the potential of typical RCs such as the ferrocene/ferrocenium pair change by tens to

Table 1. Experimental Redox Potentials Reported for the SHE in Various Solvents^{17–20}

solvent	$E_{\text{exp,SHE}}^{\text{abs}}(\text{V})$
water	4.24–4.44
acetonitrile	4.56–4.66
dimethylsulfoxide	3.83–4.04
ethanol	4.20–4.24

Table 2. Experimental Redox Potentials (in V vs SCE) for the $[\text{FeCp}_2]^{0/+}$ Couple in Various Solvents and Electrolyte Solutions^{22–25}

solvent	$\text{Li}[\text{ClO}_4]^a$	$[\text{NBu}_4][\text{ClO}_4]^b$	$[\text{NEt}_4][\text{PF}_6]^c$	$[\text{NBu}_4][\text{PF}_6]^d$
MeCN	0.31	0.40	0.38	0.40
DMSO		0.45	0.43	
DCM		0.48		0.46
DMF		0.47	0.46	0.45

^aReference 22, quarter-wave potential. ^bReference 23. ^cReference 24. ^dReference 25.

hundreds of mV with solvent or electrolyte (see Table 2 and section 5.1).^{22–25} All of these variations thus introduce significant uncertainty in the correlation between experimental and theoretical data. Removing such systematic errors would require reporting experimental and calculated redox potentials relative to a redox couple measured under the same solvent and electrolyte conditions, rather than relative to an absolute potential.

Here, we explore internal reference RCs that could be measured under the same electrolyte, solvent, and working electrode conditions, analogous to internal reference methodologies that are common practice in other fields (e.g., reports of NMR chemical shifts). For such a choice of RC, the calculated potential is

$$E_{\text{calc}}^0(\text{V vs RC}) = E_{\text{calc}}^{\text{abs}}(\text{V}) - E_{\text{calc,RC}}^{\text{abs}}(\text{V}) \quad (4)$$

where both $E_{\text{calc}}^{\text{abs}}$ and $E_{\text{calc,RC}}^{\text{abs}}$ are computed according to eq 1. Systematic uncertainties are expected to be reduced when $E_{\text{exp}}^0(\text{V vs RC})$ obtained via eq 3 is compared to $E_{\text{calc}}^0(\text{V vs RC})$ calculated via eq 4 and the following criteria are met: (i) E_{exp}^0 and $E_{\text{exp,RC}}^0$ in eq 3 are measured under identical conditions, e.g., same solvent, electrolyte, and working electrode; (ii) $E_{\text{calc}}^{\text{abs}}$ and $E_{\text{calc,RC}}^{\text{abs}}$ in eq 4 are calculated using identical conditions (e.g., same level of theory and solvent parameters); (iii) A reference transition-metal complex is chosen both for $E_{\text{exp,RC}}^0$ in eq 3 and for the calculation of $E_{\text{calc,RC}}^{\text{abs}}$ in eq 4 such that the metal lies in the same row of the periodic table as the complex used to calculate E_{calc}^0 . The rationale behind the second of these criteria is consistent with the work by Roy et al.,² who suggested to reference all computed results for redox potentials of transition metal complexes to the calculated absolute half-cell potential of ferrocene. However, we find a marked increase in performance when additional experimental and computational sources of systematic error are considered. These criteria are discussed in more detail in section 5.

3. EXPERIMENTAL METHODS

Reference compounds FeCp_2 , CoCp_2 , FeCp^*_2 , $[\text{CoCp}^*_2]^-$, $[\text{PF}_6]$, and $\text{Ir}(\text{acac})_3$ ($\text{Cp} = \eta^5\text{-cyclopentadienyl}$; $\text{Cp}^* = \eta^5\text{-1,2,3,4,5-pentamethylcyclopentadienyl}$; $\text{acac} = \text{acetylacetonate}$) were purchased from commercial sources and used as received,

and $[\text{Ru}(\text{bpy})_3][\text{PF}_6]_2$ ($\text{bpy} = 2,2'$ -bipyridine) was prepared according to a literature procedure.²⁶ Reagent grade or better acetonitrile (MeCN), dimethylsulfoxide (DMSO), and dichloromethane (DCM) were dried by passage over activated molecular sieves and degassed prior to use. Tetrabutylammonium tetrafluoroborate ($[\text{NBu}_4][\text{BF}_4]$) was recrystallized three times from ethanol and dried under a vacuum at 120 °C over P_2O_5 for 3 days. Electrochemical measurements were conducted on an IviumStat Electrochemical Interface & Impedance Analyzer from Ivium Technologies or a Pine Instruments CBP Bipotentiostat AFCBP1, and electrochemical experiments were carried out using 1 mM solutions of each reference compound in MeCN, DCM, or DMSO containing 0.1 M $[\text{NBu}_4][\text{BF}_4]$ as supporting electrolyte. Cyclic and differential pulse voltammetry experiments were performed in a beaker-type cell with a working volume of 5 mL using a standard three-electrode setup with either a glassy carbon (GC; diameter = 3 mm) or Pt (diameter = 1.6 mm) disk working electrode and a Pt wire counter electrode. For all but the $\text{Ir}(\text{acac})_3$ measurements, a homemade reference electrode consisting of Ag wire immersed in a 10 mM $\text{AgNO}_3/0.1$ M $[\text{NBu}_4][\text{BF}_4]$ electrolyte in MeCN separated from the bulk solution by a “thirsty” Vycor frit. For the $\text{Ir}(\text{acac})_3$ measurements, a homemade pseudoreference electrode was utilized in a Bioanalytical Systems MF2030 setup with a dual Vycor junction, specifically a Ag wire immersed in 0.1 M $[\text{NBu}_4][\text{BF}_4]$ in MeCN.

4. DFT COMPUTATIONAL METHODS

DFT calculations were performed by using the B3LYP exchange-correlation functional with unrestricted Kohn–Sham wave functions (UB3LYP) as implemented in the Jaguar electronic structure program.²⁷ Minimum energy configurations were obtained by using a mixed basis in which the metal centers are described by the nonrelativistic effective core potentials (ECPs) of the LACVP basis set. Five levels of theory (L1–L5) were used in an effort to compare the effect of the ligand basis set on the resulting correlation between calculated and experimental data. A summary of the levels of theory is presented in Table 3, from L1 to L5, in order of increasing

Table 3. Non-Transition-Metal Atom Basis Sets Tested in DFT/UB3LYP Calculations of Redox Potentials

level	geometry optimization	frequency calculation	single point calculation	solvation energy
L1	6-31G	6-31G		6-31G
L2	6-31G	6-31G	cc-pVTZ(-f)	cc-pVTZ(-f)
L3	6-311G*	6-311G*		6-311G*
L4	6-311G*	6-311G*	cc-pVTZ(-f)	cc-pVTZ(-f)
L5	cc-pVTZ(-f)	cc-pVTZ(-f)		cc-pVTZ(-f)

computational cost. L1 and L3 were simply based on the basis sets 6-31G and 6-311G*, respectively, while L5 was based on the Dunning's correlation-consistent triple- ζ basis set^{28–30} cc-pVTZ(-f), which includes a double set of polarization functions. Levels L2 and L4 included geometry optimizations based on the 6-31G and 6-311G* basis sets, respectively, followed by UB3LYP single point energy calculations based on the cc-pVTZ(-f) basis. The resulting correlations with experimental data are analyzed to assess the minimum computational effort necessary for quantitative predictions of redox potentials and the validity of the single-point approximation method, a commonly used method to save on computational cost, as it applies to calculations of redox potentials.

All reduction potentials were computed, according to eq 1, by calculating the free energy changes $\Delta G(\text{soln})$ associated with reduction of the complexes in solution, as follows:

$$\Delta G(\text{soln}) = \Delta G(\text{g}) + \Delta G_{\text{solv}}^{\text{P}} - \Delta G_{\text{solv}}^{\text{R}} \quad (5)$$

where $\Delta G(\text{g}) = \Delta H(\text{g}) - T\Delta S(\text{g})$ is the free energy change for the reduction reaction in the gas phase. Solvation free energies for reactants and products, $\Delta G_{\text{solv}}^{\text{R}}$ and $\Delta G_{\text{solv}}^{\text{P}}$, respectively, were computed by using the standard self-consistent reaction field approach for the gas-phase minimum energy configurations with dielectric constants of $\epsilon = 8.93, 37.5,$ and 47.24 and solvent radii of 2.33, 2.19, and 2.41 Å for DCM, MeCN, and DMSO, respectively.^{27,28}

5. RESULTS AND DISCUSSION

5.1. Method Benchmark Results. The computational results for all five levels of theory are shown alongside the experimental results in Table 4. The correlation between the computational and experimental data vs RC, where $\text{RC} = [\text{FeCp}_2]^{0/+}, [\text{Ru}(\text{bpy})_3]^{2+/3+},$ and $[\text{Ir}(\text{acac})_3]^{0/+}$ for first-second-, and third-row metal complexes, respectively, is shown in Figure 1 for theory levels L1, L3, and L5. The distributions in $E_{L_n}^0 - E_{\text{exp}}^0$ for all levels of theory $L_n, n = 1-5,$ are shown in Figure 2 with means and standard deviations given in Table 5. The L3 level of theory, though not the most computationally expensive, is the best performing in terms of standard deviation with respect to the experimental data. This level gives a standard deviation of 56 mV for the 12 of 18 couples that lie in the first row, compared to 150 and 90 mV for the L1 and L5 levels of theory. When the same $[\text{FeCp}_2]^{0/+}$ RC is used and extended to all couples as suggested by Roy et al.,² the standard deviation rises to 148 mV for the L3 level of theory. Though this standard deviation is an improvement over previous reports of method performance, which we attribute to reductions in systematic error in the experimental data, it still marks a sharp decrease in performance compared to the first-row couples alone. However, when a RC with a similar ECP is used, the values are comparable to the first-row statistics. The L3 level of theory yields a standard deviation of 64 mV and a mean of -2 mV for all 18 couples.

In addition to evaluating the impact of the basis set on the correlation between measured and calculated redox potentials as a means of finding accurate low-computational-cost methods, we evaluated the use of a single-point energy calculation to approximate a redox potential calculated at a higher level of theory. In theory level L2 (L4), we used the geometry obtained in theory level L1 (L3) and used a single point correction at the LACVP/cc-pVTZ(-f) level of theory to approximate a level L5 redox potential calculation. The correlations between redox potential calculations involving a single-point calculation and those obtained strictly at the level L5 theory are shown in Figure 4. The means and standard deviations for the 25 data points (see Tables 4 and 7) are 54 and 97 mV for $E_{L2}^0 - E_{L5}^0$ and 30 and 66 mV for $E_{L4}^0 - E_{L5}^0$, respectively. The better correlation between the L4 and L5 levels of theory can be attributed to the fact that, unlike the 6-31G basis set, the 6-311G* and cc-pVTZ(-f) basis sets both contain polarization functions. However, in terms of comparisons with experiment, L2 shows a marked increase in performance compared to L1 (see Figure 2 and Table 5). Depending on the size and time constraints of the calculation, geometries based on the LACVP/

Table 4. Measured E_{exp}^0 and Calculated $E_{L_n}^0$ Redox Potentials in V vs RC of Benchmark Transition-Metal Complexes^{25,31–39} for Five Different Levels of Theory

couple	solvent	RC ^a	spin ^b	E_{exp}^0	E_{L1}^0	E_{L2}^0	E_{L3}^0	E_{L4}^0	E_{L5}^0
[CoCp ₂] ^{0/+}	MeCN	[FeCp ₂] ^{0/+} (RC1A)	d/s	-1.322 ^{c,d}	-1.267	-1.351	-1.295	-1.278	-1.257
[CoCp ₂] ^{0/+}	DCM	[FeCp ₂] ^{0/+} (RC1K)	d/s	-1.35 ^{c,e}	-1.271	-1.354	-1.298	-1.280	-1.261
[NiCp ₂] ^{0/+}	MeCN	[FeCp ₂] ^{0/+} (RC1C)	t/d	-0.47 ^{c,f}	-0.505	-0.516	-0.386	-0.304	-0.318
[NiCp ₂] ^{0/+}	DCM	[FeCp ₂] ^{0/+} (RC1K)	t/d	-0.42 ^{c,e}	-0.503	-0.512	-0.391	-0.306	-0.306
[RuCp ₂] ^{0/+}	DCM	[Ru(bpy) ₃] ^{2+/3+} (RC2B)	s/d	-0.372 ^{g,h}	-0.124	-0.408	-0.457	-0.516	-0.255
[OsCp ₂] ^{0/+}	DCM	[Ir(acac) ₃] ^{0/+} (RC3B)	s/d	-0.310 ^{i,j}	-0.644	-0.287	-0.246	-0.209	-0.343
[FeCp* ₂] ^{0/+}	MeCN	[FeCp ₂] ^{0/+} (RC1A)	s/d	-0.539 ^{c,d}	-0.675	-0.634	-0.565	-0.542	-0.585
[FeCp* ₂] ^{0/+}	DMSO	[FeCp ₂] ^{0/+} (RC1G)	s/d	-0.468 ^{c,k}	-0.672	-0.631	-0.562	-0.541	-0.589
[FeCp* ₂] ^{0/+}	DCM	[FeCp ₂] ^{0/+} (RC1K)	s/d	-0.532 ^{c,e}	-0.711	-0.665	-0.596	-0.574	-0.616
[CoCp* ₂] ^{0/+}	MeCN	[FeCp ₂] ^{0/+} (RC1A)	d/s	-1.883 ^{c,d}	-1.932	-1.935	-1.945	-1.921	-1.883
[CoCp* ₂] ^{0/+}	DCM	[FeCp ₂] ^{0/+} (RC1K)	d/s	-1.97 ^{c,e}	-1.969	-1.968	-1.977	-1.955	-1.916
[NiCp* ₂] ^{0/+}	DCM	[FeCp ₂] ^{0/+} (RC1K)	t/d	-1.22 ^{c,e}	-1.376	-1.271	-1.197	-1.164	-1.194
[RuCp* ₂] ^{0/+}	DCM	[Ru(bpy) ₃] ^{2+/3+} (RC2B)	s/d	-0.872 ^{h,l}	-0.759	-0.972	-0.896	-0.989	-0.798
[OsCp* ₂] ^{0/+}	DCM	[Ir(acac) ₃] ^{0/+} (RC3B)	s/d	-0.700 ^{h,l,m}	-0.974	-0.500	-0.626	-0.606	-0.666
[Fe(bpy) ₃] ^{2+/3+}	MeCN	[FeCp ₂] ^{0/+} (RC1D)	s/d	0.63 ⁿ	0.157	0.441	0.603	0.619	0.538
[Co(bpy) ₃] ^{2+/3+}	MeCN	[FeCp ₂] ^{0/+} (RC1D)	d/s	0.12 ⁿ	-0.406	-0.003	0.044	0.108	0.048
[Os(bpy) ₃] ^{2+/3+}	MeCN	[Ir(acac) ₃] ^{0/+} (RC3A)	s/d	-0.319 ⁿ	-0.204	-0.114	-0.203	-0.113	-0.099
[Ir(bpy) ₃] ^{2+/3+}	MeCN	[Ir(acac) ₃] ^{0/+} (RC3A)	d/s	-1.938 ^o	-1.922	-1.964	-1.985	-1.984	-1.897

^aRC measurement conditions given in Table 6. ^bs = singlet, d = doublet, t = triplet. ^cMeasured under identical conditions as RC. ^dThis work. ^eReference 31. ^fReference 32. ^g $E_{\text{exp},[\text{RuCp}_2]^{0/+}}^0 = 0.56$ V vs [FeCp₂]^{0/+} (RC1L; ref 40). ^h $E_{\text{exp},[\text{Ru}(\text{bpy})_3]^{2+/3+}}^0 = 0.932$ V vs [FeCp₂]^{0/+} (RC1H and RC2B; this work). ⁱ $E_{\text{exp},[\text{OsCp}_2]^{0/+}}^0 = 0.36$ V vs [FeCp₂]^{0/+} (RC1L; ref 40). ^j $E_{\text{exp},[\text{Ir}(\text{acac})_3]^{0/+}}^0 = 0.670$ V vs [FeCp₂]^{0/+} (RC1I and RC3B; this work). ^kReference 33. ^l $E_{\text{exp},[\text{RuCp}^*_2]^{0/+}}^0 = 0.06$ V vs [FeCp₂]^{0/+} (RC1K; refs 34 and 31). ^m $E_{\text{exp},[\text{OsCp}^*_2]^{0/+}}^0 = -0.09$ V vs [RuCp*₂]^{0/+}, supporting electrolyte conditions not reported (ref 36). ⁿ[M(bpy)₃]^{2+/3+} from ref 37 and [FeCp₂]^{0/+} from ref 23 (RC1D) with similar conditions. ^oReference 39, measured under different electrolyte conditions (0.1 M [NEt₄][ClO₄]) than RC.

6-31G level of theory followed by single-point energy calculations can lead to good comparisons with experiment based on means and standard deviations on the order of -21 and 117 mV, respectively. For a moderate increase in computational cost, however, calculations carried out strictly at the LACVP/6-311G* level of theory give the best performance of the levels of theory studied.

5.2. Reference Redox Couples. There are several merits to using the proposed reference redox systems, as recommended by the IUPAC.²¹ The main advantage is that we avoid the use of aqueous reference electrodes that might generate a liquid junction potential, such as the saturated calomel electrode (SCE) or the standard hydrogen electrode. Even nonaqueous reference electrodes based on the same solvent are prone to issues of reproducibility due to electrode surface chemistry.²¹ These factors can contribute to discrepancies on the order of tens to hundreds of millivolts, even when comparing measurements reported under the same electrolyte and solvent conditions. Using reference redox couples that are free of liquid junction potentials and electrode surface chemistry effects can thus provide results that are more consistent over a wide range of experimental conditions. In addition to these experimental considerations, the use of internal reference redox couples is also expected to remove systematic uncertainty at the computational level. This is attributed to the fact that the accuracy of E_{calc}^0 (V vs RC) is as equally dependent on the reference value as it is on the calculated absolute potential of the couple being studied (eqs 2 and 4). When a RC is used, the reference can be calculated directly instead of relying on eq 2 and an external reference reported elsewhere. The direct calculation thus eliminates potential sources of systematic error (e.g., see Table 1).

Several previous studies have focused on finding the appropriate functional and size of the basis set to get accurate

estimates of absolute redox potentials.^{1–9} Here we note that when the deviations between calculated and experimental values are systematic, referencing the calculated potentials to a redox couple calculated with the same functional and basis set, as in eq 4, should remove systematic deviations and yield better accuracy even at a low computational cost when using modest basis sets. Table 6 reports the values of experimental redox potentials $E_{\text{exp,RC}}^0$ (V vs RE) for the reference redox couples depicted in Scheme 2 under various electrolyte, working electrode, and solvent conditions. Table 7 gives the corresponding values of calculated absolute redox potentials $E_{\text{calc,RC}}^{\text{abs}}$ (V), obtained according to the levels of theory described in section 4.

[FeCp₂]^{0/+} is a well-known RC for nonaqueous solutions with a host of available electrochemical data under a wide variety of experimental conditions (Table 6; RC1A through RC1L).^{23,25,31–33,38,40} Several previous studies have explored first principle methods for calculating redox potentials, using [FeCp₂]^{0/+} as a reference RC, and have been most successful at predicting potentials for complexes of first-row transition metals. However, calculations for second- and third-row transition metal complexes have proven more challenging. Row-specific discrepancies suggest systematic computational errors likely due to the choice of basis sets, pseudopotentials, or solvation models when comparing the redox properties of transition metals with different valence shells. In the present work, these systematic uncertainties are addressed by choosing reference couples with metal centers in the same row as the system of interest.

[FeCp₂]^{0/+} is the most common choice for a first-row reference RC. Choosing references for the second and third row, however, is a bit more challenging. Available electrochemical data is not as abundant and most complexes, including the metallocene analogues, are only reproducible under limited

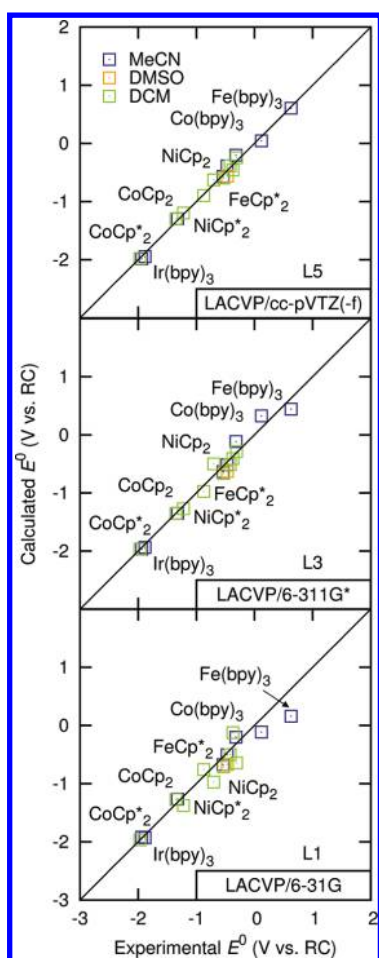


Figure 1. Correlation between measured E_{exp}^0 and calculated E_{Ln}^0 redox potentials in V vs RC, where RC = $[\text{FeCp}_2]^{0/+}$, $[\text{Ru}(\text{bpy})_3]^{2+/3+}$, and $[\text{Ir}(\text{acac})_3]^{0/+}$ for first-, second-, and third-row transition-metal complexes, respectively, using L1, L3, and L5 levels of theory. Sources of experimental data are given in Table 4.

experimental conditions. Hill et al. demonstrated that, in solutions of DCM and $[\text{NBu}_4][\text{B}(\text{Ar}^{\text{F}})_4]$ ($\text{Ar}^{\text{F}} = 3,5$ -bistrifluoromethylphenyl), ruthenocene and osmocene each exhibit a single, quasi-reversible oxidation.⁴⁰ However, oxidations of these metallocenes in MeCN are reported to be irreversible two- and one-electron processes, respectively.³⁸ DC and AC polarography show that the $[\text{RhCp}_2]^{0/+}$ couple can be highly reversible, though rhodocene has a lifetime on the order of seconds and is unstable at room temperature on the cyclic voltammetry time scale.⁴¹ To avoid these difficulties, we have chosen to use two relatively well-known systems, including $[\text{Ru}(\text{bpy})_3]^{2+/3+}$ which has become popular due to its use in photoredox catalysis and artificial photosynthesis^{42–44} and $[\text{Ir}(\text{acac})_3]^{0/+}$ which is often used as a precursor for complexes relevant to organic light-emitting diodes.^{45–47} Both systems show reversible or quasi-reversible peaks in both DCM and MeCN.

5.3. Solvent Polarity and Supporting Electrolyte. The impact of the solvent on the potential of both the reference and the couple being studied is often underestimated. Figure 5 shows cyclic voltammograms of the $[\text{FeCp}_2]^{0/+}$ couple measured in 0.1 M $[\text{NBu}_4][\text{BF}_4]$ in MeCN, DMSO, and DCM solvents. Values of the redox potential are 0.084, 0.033, and 0.210 V vs Ag/AgNO_3 for the three solvents, respectively.

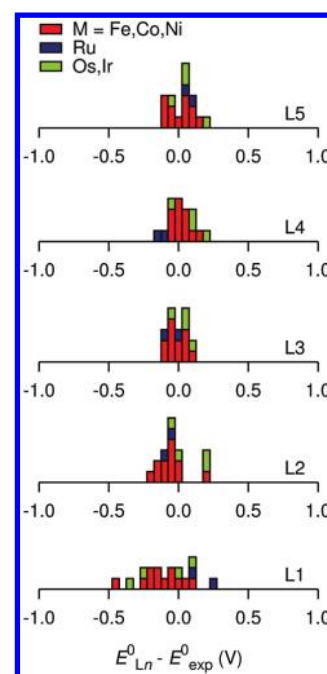


Figure 2. Distribution in $E_{\text{Ln}}^0 - E_{\text{exp}}^0$ for the five levels of theory, based on experimental data and calculations vs RC, where RC = $[\text{FeCp}_2]^{0/+}$, $[\text{Ru}(\text{bpy})_3]^{2+/3+}$, and $[\text{Ir}(\text{acac})_3]^{0/+}$ for first- (red), second- (navy), and third-row (green) metal complexes, respectively. Means and standard deviations are given in Table 5.

Table 5. Means μ and Standard Deviations σ of the Distributions in $E_{\text{Ln}}^0 - E_{\text{exp}}^0$ (see Figure 2) for Calculations Performed at the Five Levels of Theory L_n

level	M = Fe, Co, Ni ^a		all metals ^a		all metals ^b	
	μ (mV)	σ (mV)	μ (mV)	σ (mV)	μ (mV)	σ (mV)
L5	7	90	-101	182	30	92
L4	24	69	-75	167	21	94
L3	-12	56	-100	148	-2	64
L2	-54	101	-152	176	-21	117
L1	-118	150	-228	205	-85	181

^a $[\text{FeCp}_2]^{0/+}$ reference couple. ^bUsing a reference couple in the same row as shown in Table 6.

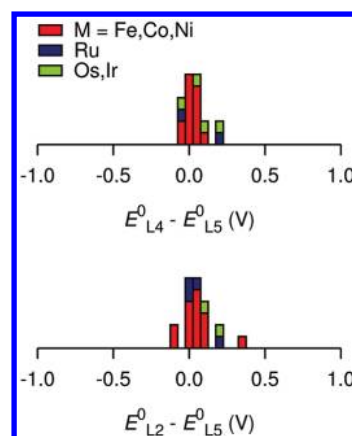


Figure 3. Deviation between UB3LYP redox potential calculations obtained strictly at the LACVP/cc-pVTZ(-f) level of theory (E_{L5}^0) and approximate calculations using minimum energy structures obtained at the LACVP/6-31G (E_{L2}^0) and LACVP/6-311G* (E_{L4}^0) levels with LACVP/cc-pVTZ(-f) single-point energy corrections.

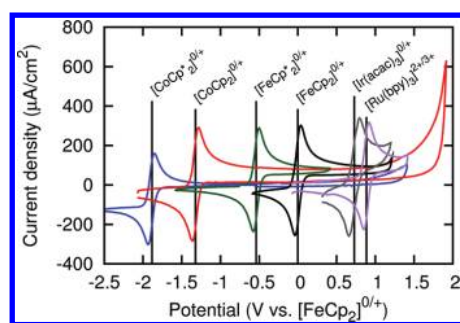


Figure 4. Cyclic voltammograms of $[\text{CoCp}^*_2]^{0/+}$ (blue), $[\text{CoCp}_2]^{0/+}$ (red), $[\text{FeCp}^*_2]^{0/+}$ (green), $[\text{FeCp}_2]^{0/+}$ (black), $[\text{Ir}(\text{acac})_3]^{0/+}$ (gray), and $[\text{Ru}(\text{bpy})_3]^{2+/3+}$ (purple) couples in 0.1 M $[\text{NBu}_4][\text{BF}_4]$ in acetonitrile (100 mV s^{-1} scan rate; $T = 25^\circ\text{C}$; current density of $[\text{Ir}(\text{acac})_3]^{0/+}$ is reduced by a factor of 3).

The experimentally observed shift of 177 mV in the oxidation potential for the $[\text{FeCp}_2]^{0/+}$ couple in DCM relative to DMSO emphasizes the importance of accounting for solvent effects. This shift is also reflected in the calculations with a difference of 179 mV in the calculated absolute redox potential of the $[\text{FeCp}_2]^{0/+}$ couple in DMSO and DCM using the L3 level of theory. This gives an estimate of the potential error introduced when a solvent-independent reference electrode or couple is used to compare experimental and computational redox potentials. These data also provide an example of how well self-consistent reaction-field methods can account for solvent effects in electrochemistry calculations.

The role of the supporting electrolyte should also be considered carefully in electrochemical calculations. Typical experimental concerns related to the electrolyte, including ionic conductivity and reactivity, do not enter into the explicit calculation of a redox potential. In addition, although the dielectric constant of the medium can depend on the concentration of the electrolyte,⁴⁸ typical concentrations are considered low enough that the electrolyte is often assumed to have a negligible effect on the calculations. However, ion

pairing with supporting electrolyte counterions can become favorable when the complex is highly charged, as in the case of the $[\text{Ru}(\text{bpy})_3]^{2+/3+}$ couple, depending on the polarity of the solvent. In this case, we find that explicit supporting electrolyte counterions must be considered in the calculation. It is also important to justify the use of explicit counterions because geometry optimizations are typically performed in the nonpolar gas phase, which would give results that are biased toward ion pairing.

The measured oxidation potential of the $[\text{Ru}(\text{bpy})_3]^{2+/3+}$ couple is higher in DCM than in MeCN by 174 mV vs Ag/AgNO_3 . When two explicit $[\text{BF}_4]^-$ counterions are included in the DCM case (see Figure 6), the calculated difference in absolute potential is 102 mV at the L3 level of theory. This is to be compared with a shift of 574 mV when ion pairing is neglected. The correction to $E_{\text{calc}}^{\text{abs}}$ due to ion pairing is 472 mV in low-polarity DCM ($\epsilon = 8.93$), while it is only 38 mV in MeCN ($\epsilon = 37.5$). These results emphasize the importance of including explicit counterions for highly charged species in low-polarity solvents, while demonstrating how ion-pairing effects are drastically reduced with a relatively high-polarity solvent, even when the comparison is based on geometries optimized in the nonpolar gas phase. For these reasons, we use the explicit counterion results for the $[\text{Ru}(\text{bpy})_3]^{2+/3+}$ couple in DCM, but not in MeCN, in which case ion pairing is not expected to be a significant factor.

5.4. Benchmark Redox Couples. The benchmark redox couples used in this work are shown in Scheme 2. All reduced and oxidized forms of the complexes were determined to be either singlets or doublets except for NiCp_2 and NiCp^*_2 , which have triplet states that are lower in gas-phase free energy than their singlet states by 23.4 and 16.6 kcal/mol, respectively, as calculated at the L3 level of theory and indicated in Table 4. All measured redox potentials for these complexes are given in Tables 4 and 6. The redox couples measured in the present work are referenced to a RC measured on the same system, and therefore with the same working electrode and supporting electrolyte and solvent conditions. Values obtained from the literature were obtained in the same manner, when possible.

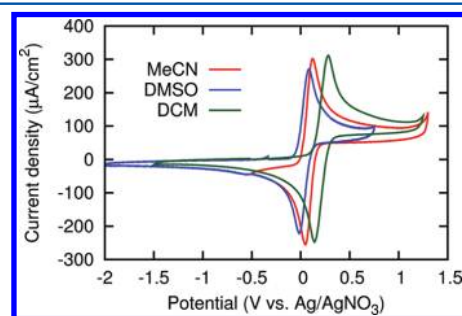
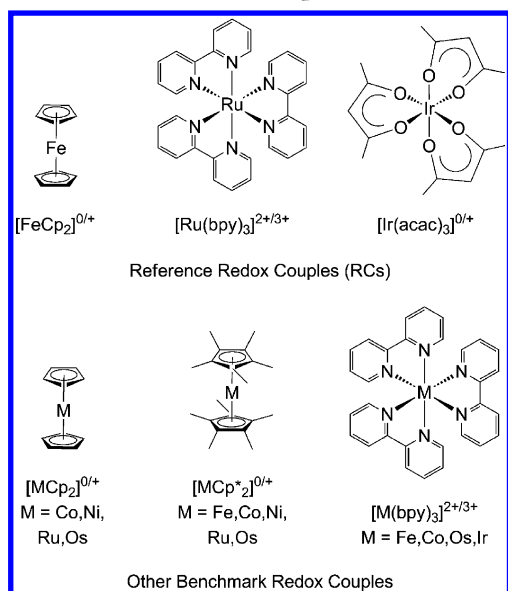
Table 6. Measured Redox Potentials $E_{\text{exp,RC}}^0$ (V vs RE) of the Reference Redox Couples in Various Measurement Conditions

	reference couple	solvent	supporting electrolyte anion ^a	working electrode	reference electrode (RE)	$E_{\text{exp,RC}}^0$ (V vs RE)
RC1A	$[\text{FeCp}_2]^{0/+}$	MeCN	$[\text{BF}_4]^-$	GC	Ag/AgNO_3	0.084 ^{b,c}
RC1B	$[\text{FeCp}_2]^{0/+}$	MeCN	$[\text{BF}_4]^-$	GC	Ag wire	0.498 ^{b,c}
RC1C	$[\text{FeCp}_2]^{0/+}$	MeCN	$[\text{BF}_4]^-$	Pt	SCE	0.48 ^{d,e,f}
RC1D	$[\text{FeCp}_2]^{0/+}$	MeCN	$[\text{ClO}_4]^-$	Pt	SCE	0.40 ^{g,h}
RC1E	$[\text{FeCp}_2]^{0/+}$	MeCN	$[\text{PF}_6]^-$		SCE	0.40 ^{b,i}
RC1F	$[\text{FeCp}_2]^{0/+}$	DMSO	$[\text{BF}_4]^-$	GC	Ag/AgNO_3	0.033 ^{b,c}
RC1G	$[\text{FeCp}_2]^{0/+}$	DMSO	$[\text{ClO}_4]^-$	Au, Pt, or GC	$\text{Ag}/\text{AgCl}/\text{KCl}$ (sat.)	0.505 ^{b,j}
RC1H	$[\text{FeCp}_2]^{0/+}$	DCM	$[\text{BF}_4]^-$	GC	Ag/AgNO_3	0.210 ^{b,c}
RC1I	$[\text{FeCp}_2]^{0/+}$	DCM	$[\text{BF}_4]^-$	Pt	Ag wire	0.548 ^{b,c}
RC1J	$[\text{FeCp}_2]^{0/+}$	DCM	$[\text{ClO}_4]^-$	Pt	SCE	0.48 ^{g,h}
RC1K	$[\text{FeCp}_2]^{0/+}$	DCM			SCE	0.49 ^{b,k}
RC1L	$[\text{FeCp}_2]^{0/+}$	DCM	$[\text{B}(\text{Ar}^F)_4]^-$		Ag/AgCl , 1 M KCl	0.47 ^{b,l}
RC2A	$[\text{Ru}(\text{bpy})_3]^{2+/3+}$	MeCN	$[\text{BF}_4]^-$	GC	Ag/AgNO_3	0.968 ^{b,c}
RC2B	$[\text{Ru}(\text{bpy})_3]^{2+/3+}$	DCM	$[\text{BF}_4]^-$	GC	Ag/AgNO_3	1.142 ^{g,c}
RC3A	$[\text{Ir}(\text{acac})_3]^{0/+}$	MeCN	$[\text{BF}_4]^-$	GC	Ag wire	1.226 ^{b,c}
RC3B	$[\text{Ir}(\text{acac})_3]^{0/+}$	DCM	$[\text{BF}_4]^-$	Pt	Ag wire	1.218 ^{b,c}

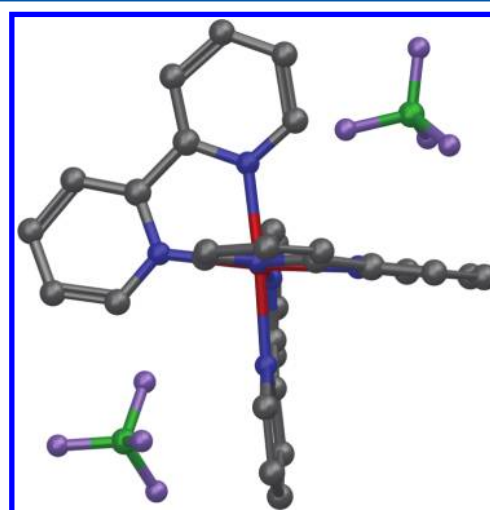
^a0.1 M supporting electrolyte with $[\text{NBu}_4]^+$ cation. ^bCyclic voltammetry. ^cThis work. ^dRotating disk electrode voltammetry. ^eReference 38. ^fReference 32. ^gDifferential pulse polarography. ^hReference 23. ⁱReference 25, working electrode not reported. ^jReference 33. ^kReference 31, working electrode and supporting electrolyte not reported though later work (refs 34 and 35) suggests 0.1 M $[\text{NBu}_4][\text{PF}_6]$. ^lReference 40, working electrode not reported.

Table 7. Absolute Redox Potentials E_{Ln}^{abs} (V) of the Reference Redox Couples Used in This Work Calculated at the Five Different Levels of Theory L_n

RC	solvent	E_{L1}^{abs}	E_{L2}^{abs}	E_{L3}^{abs}	E_{L4}^{abs}	E_{L5}^{abs}
$[\text{FeCp}_2]^{0/+}$	MeCN	5.172	5.183	5.135	5.086	5.086
$[\text{FeCp}_2]^{0/+}$	DMSO	5.160	5.172	5.124	5.077	5.078
$[\text{FeCp}_2]^{0/+}$	DCM	5.340	5.350	5.303	5.255	5.256
$[\text{Ru}(\text{bpy})_3]^{2+/3+}$	MeCN	5.521	5.802	5.797	5.787	5.800
$[\text{Ru}(\text{bpy})_3]^{2+/3+}$	DCM	5.589	5.910	5.899	5.930	5.730
$[\text{Ir}(\text{acac})_3]^{0/+}$	MeCN	5.383	5.526	5.608	5.530	5.480
$[\text{Ir}(\text{acac})_3]^{0/+}$	DCM	5.924	5.598	5.685	5.606	5.543

Scheme 2. Benchmark Redox Couples Studied in This Work**Figure 5.** Cyclic voltammograms of the $[\text{FeCp}_2]^{0/+}$ couple in 0.1 M $[\text{NBu}_4][\text{BF}_4]$ in acetonitrile (red), dimethylsulfoxide (blue), and dichloromethane (green) solvents (100 mV s^{-1} scan rate; $T = 25^\circ\text{C}$).

This was possible for all of the first-row couples reported in Table 4, since many electrochemical studies report potentials versus $[\text{FeCp}_2]^{0/+}$. The second- and third-row couples, for which limited data is available, were referenced to $[\text{FeCp}_2]^{0/+}$ under similar conditions. These data were then compared to the RC vs $[\text{FeCp}_2]^{0/+}$ measured in the present work. In certain cases, the electrolyte conditions or working electrode were not identical or reported, as indicated in Tables 4 and 6. In particular, the potential for the $[\text{Ir}(\text{bpy})_3]^{2+/3+}$ couple,³⁹ which was reported in 0.1 M $[\text{NEt}_4][\text{ClO}_4]$, is based on a measurement of $[\text{FeCp}_2]^{0/+}$ in 0.1 M $[\text{NBu}_4][\text{ClO}_4]$,²³ and the supporting electrolyte conditions for the $[\text{OsCp}^*_2]^{0/+}$ were not reported. In addition, the data that is based on couples from multiple sources in the literature, i.e., differing

**Figure 6.** Optimized net-neutral geometry of $[\text{Ru}(\text{bpy})_3]^{2+}$ with two explicit $[\text{BF}_4]^-$ counterions obtained at the L3 level of theory. Hydrogens removed for clarity. Element color key: B (green); C (gray); N (blue); F (purple); Ru (red).

experimental setups, is indicated in the table. Since the working electrodes are not always reported, some systematic error due to differing working electrodes may exist, as discussed in section 5.2. However, the criteria for minimizing systematic error seem to be met for the present data set based on the correlation with calculated results discussed in section 5.1.

6. CONCLUSIONS

We have demonstrated a low-computational-cost method for accurate calculations of redox potentials of transition-metal complexes. As in previous first-principle computational studies, we have assessed the degree to which the level of theory affects the robustness of the methodology. We found that the correlation between calculated and experimental data was best when using three important guidelines for reducing systematic error: (i) the use of an experimental reference redox couple measured under identical experimental conditions; (ii) the use of a computational reference redox couple calculated at the same level of theory (which serves the dual purpose of removing computational systematic error while precluding the use of an external measurement of the absolute potential of a reference electrode that can introduce additional experimental systematic error); (iii) the restriction that the metal centers of the electrochemically active complex and the reference couple belong to the same row of the periodic table. This ensures reduction in computational systematic error, since the metals in each row share a common set of core electrons and there is therefore better agreement of the pseudopotentials of the metal basis set. Following these guidelines, we demonstrated a standard

deviation of 64 mV and a mean of -2 mV for the 18 benchmark redox potentials and seven reference potentials calculated at the DFT/UB3LYP level of theory with LACVP and 6-311G* basis sets, which, though not the largest, is the best-performing level of theory investigated in this benchmark study. In this way, accurate calculations of redox potentials are obtained at relatively low computational cost, even for transition metal complexes in the second and third rows for which poor performance has been previously reported.

■ ASSOCIATED CONTENT

■ Supporting Information

Energy contributions and absolute redox potentials for all reported calculations and geometries as well as geometries for all benchmark transition-metal complexes. This material is available free of charge via the Internet at <http://pubs.acs.org>.

■ AUTHOR INFORMATION

Corresponding Author

*E-mail: steven.konezny@yale.edu (S.J.K.); victor.batista@yale.edu (V.S.B.).

Notes

The authors declare no competing financial interest.

■ ACKNOWLEDGMENTS

This work has been supported as part of the Center for Electrocatalysis, Transport Phenomena, and Materials for Innovative Energy Storage, an Energy Frontier Research Center funded by the U.S. Department of Energy, Office of Science, Office of Basic Energy Sciences under Award Number DE-SC0001055.

■ REFERENCES

- (1) Baik, M.-H.; Friesner, R. A. *J. Phys. Chem. A* **2002**, *106*, 7407–7412.
- (2) Roy, L. E.; Jakubikova, E.; Guthrie, M. G.; Batista, E. R. *J. Phys. Chem. A* **2009**, *113*, 6745–6750.
- (3) Chiorescu, I.; Deubel, D. V.; Arion, V. B.; Keppler, B. K. *J. Chem. Theory Comput.* **2008**, *4*, 499–506.
- (4) Li, J.; Fisher, C. L.; Chen, J. L.; Bashford, D.; Noodleman, L. *Inorg. Chem.* **1996**, *35*, 4694–4702.
- (5) Moens, J.; Geerlings, P.; Roos, G. *Chem.—Eur. J.* **2007**, *13*, 8174–8184.
- (6) Moens, J.; Jaque, P.; De Proft, F.; Geerlings, P. *J. Phys. Chem. A* **2008**, *112*, 6023–6031.
- (7) Uudsemaa, M.; Tamm, T. *J. Phys. Chem. A* **2003**, *107*, 9997–10003.
- (8) Galstyan, A.; Knapp, E.-W. *J. Comput. Chem.* **2009**, *30*, 203–211.
- (9) de Groot, M. T.; Koper, M. T. M. *Phys. Chem. Chem. Phys.* **2008**, *10*, 1023–1031.
- (10) Wang, T.; Brudvig, G.; Batista, V. S. *J. Chem. Theory Comput.* **2010**, *6*, 755–760.
- (11) Wang, T.; Brudvig, G. W.; Batista, V. S. *J. Chem. Theory Comput.* **2010**, *6*, 2395–2401.
- (12) Moens, J.; Roos, G.; Jaque, P.; De Proft, F.; Geerlings, P. *Chem.—Eur. J.* **2007**, *13*, 9331–9343.
- (13) Roy, L. E.; Batista, E. R.; Hay, P. J. *Inorg. Chem.* **2008**, *47*, 9228–9237.
- (14) Wang, T.; Friesner, R. A. *J. Phys. Chem. C* **2009**, *113*, 2553–2561.
- (15) Tsai, M.-K.; Rochford, J.; Polyansky, D. E.; Wada, T.; Tanaka, K.; Fujita, E.; Muckerman, J. T. *Inorg. Chem.* **2009**, *48*, 4372–4383.
- (16) Ayala, R.; Sprik, M. *J. Chem. Theory Comput.* **2006**, *2*, 1403–1415.
- (17) Trasatti, S. *Pure Appl. Chem.* **1986**, *58*, 955–966.
- (18) Kelly, C. P.; Cramer, C. J.; Truhlar, D. G. *J. Phys. Chem. B* **2006**, *110*, 16066–16081.
- (19) Kelly, C. P.; Cramer, C. J.; Truhlar, D. G. *J. Phys. Chem. B* **2007**, *111*, 408–422.
- (20) Fawcett, W. R. *Langmuir* **2008**, *24*, 9868–9875.
- (21) Gritzner, G.; Kuta, J. *Pure Appl. Chem.* **1984**, *56*, 461–466.
- (22) Kuwana, T.; Bublit, D. E.; Hoh, G. *J. Am. Chem. Soc.* **1960**, *82*, 5811–5817.
- (23) Chang, D.; Malinski, T.; Ulman, A.; Kadish, K. M. *Inorg. Chem.* **1984**, *23*, 817–824.
- (24) Chang, J. P.; Fung, E. Y.; Curtis, J. C. *Inorg. Chem.* **1986**, *25*, 4233–4241.
- (25) Connelly, N. G.; Geiger, W. E. *Chem. Rev.* **1996**, *96*, 877–910.
- (26) Fetterolf, M. L.; Offen, H. W. *Inorg. Chem.* **1987**, *26*, 1070–1072.
- (27) Jaguar, version 7.7; Schrodinger, LLC: New York, 2010.
- (28) Dunning, T. H. *J. Chem. Phys.* **1989**, *90*, 1007–1023.
- (29) Kendall, R. A.; Dunning, T. H.; Harrison, R. J. *J. Chem. Phys.* **1992**, *96*, 6796–6806.
- (30) Woon, D. E.; Dunning, T. H. *J. Chem. Phys.* **1993**, *98*, 1358–1371.
- (31) Kölle, U.; Khouzami, F. *Angew. Chem., Int. Ed.* **1980**, *19*, 640–641.
- (32) Gubin, S. P.; Smirnova, S. A.; Denisovich, L. I. *J. Organomet. Chem.* **1971**, *30*, 257–265.
- (33) Noviandri, I.; Brown, K. N.; Fleming, D. S.; Gulyas, P. T.; Lay, P. A.; Masters, A. F.; Phillips, L. *J. Phys. Chem. B* **1999**, *103*, 6713–6722.
- (34) Kölle, U.; Salzer, A. *J. Organomet. Chem.* **1983**, *243*, C27–C30.
- (35) Kölle, V.; Grub, J. *J. Organomet. Chem.* **1985**, *289*, 133–139.
- (36) O'Hare, D.; Green, J. C.; Chadwick, T. P.; Miller, J. S. *Organometallics* **1988**, *7*, 1335–1342.
- (37) Saji, T.; Aoyagui, S. *J. Electroanal. Chem. Interfacial Electrochem.* **1975**, *60*, 1–10.
- (38) Gubin, S. P.; Smirnova, S. A.; Denisovich, L. I.; Lubovich, A. A. *J. Organomet. Chem.* **1971**, *30*, 243–255.
- (39) Kahl, J. L.; Hanck, K. W.; DeArmond, K. *J. Phys. Chem.* **1978**, *82*, 540–545.
- (40) Hill, M. G.; Lamanna, W. M.; Mann, K. R. *Inorg. Chem.* **1991**, *30*, 4687–4690.
- (41) El Murr, N.; Sheats, J. E.; Geiger, W. E.; Holloway, J. D. L. *Inorg. Chem.* **1979**, *18*, 1443–1446.
- (42) Zeitler, K. *Angew. Chem., Int. Ed.* **2009**, *48*, 9785–9789.
- (43) Bard, A. J.; Fox, M. A. *Acc. Chem. Res.* **1995**, *28*, 141–145.
- (44) Juris, A.; Balzani, V.; Barigelletti, F.; Campagna, S.; Belser, P.; von Zelewsky, A. *Coord. Chem. Rev.* **1988**, *84*, 85–277.
- (45) Tsuboyama, A.; Iwawaki, H.; Furugori, M.; Mukaide, T.; Kamatani, J.; Igawa, S.; Moriyama, T.; Miura, S.; Takiguchi, T.; Okada, S.; Hoshino, M.; Ueno, K. *J. Am. Chem. Soc.* **2003**, *125*, 12971–12979.
- (46) Lamansky, S.; Djurovich, P.; Murphy, D.; Abdel-Razzaq, F.; Kwong, R.; Tsyba, I.; Bortz, M.; Mui, B.; Bau, R.; Thompson, M. E. *Inorg. Chem.* **2001**, *40*, 1704–1711.
- (47) Wong, K.-T.; Chen, Y.-M.; Lin, Y.-T.; Su, H.-C.; Wu, C.-c. *Org. Lett.* **2005**, *7*, 5361–5364.
- (48) Bao, D.; Millare, B.; Xia, W.; Steyer, B. G.; Gerasimenko, A. A.; Ferreira, A.; Contreras, A.; Vullev, V. I. *J. Phys. Chem. A* **2009**, *113*, 1259–1267.